PERGAMON

International Journal of Solids and Structures 36 (1999) 2379–2395

INTERNATIONAL JOURNAL OF SOLIDS and STRUCTURES

Experimental and theoretical predictions of first-ply failure strength of laminated composite plates

T. Y. Kam*, F. M. Lai

Department of Mechanical Engineering, National Chiao Tung University, Hsin-Chu 30050 Taiwan, People's Republic of China

Received 4 April 1997; received in revised form 23 February 1998

Abstract

Experimental and theoretical methods are presented to study the first-ply failure strength of laminated composite plates under different loading conditions. An acoustic emission technique is used to measure the energy released in the plates during the failure process. The first-ply failure strength of the plates is then identified via the energy vs load diagrams which are constructed on the basis of the measured acoustic emissions. A finite element analysis, which is constructed on the basis of the layerwise linear displacement theory, and the Tsai–Wu failure criterion are used to predict the first-ply failure strength of the plates. The comparison between the experimental and theoretical results shows good agreement.

Keywords: Laminates; Composite materials; Failure; Acoustic emission; Finite element; Static test; Strength

1. Introduction

Laminated composite materials have become an important engineering material for the construction of mechanical, aerospace, marine and automotive structures in recent years. In spite of their wide application, the design of reliable laminated composite structures is still a goal to be achieved. For reliability assurance, the realistic failure processes of laminated composite structures and the maximum loads that the structures can sustain before failure occurs, must be fully understood and accurately predicted. In general, the concept of first-ply failure has been used as a criterion for the design of laminated composite structures. Thus, the determination of accurate first-ply failure loads of laminated composite structures has become an important topic of research. Recently, several researchers have studied the first-ply failure strength of laminated composite plates. For instance, Turvey (1980a, b, c, 1981) used analytical methods to evaluate the linear and nonlinear first-ply failure loads of simply-supported symmetrically and anti-symmetrically

* Corresponding author. Fax: 00-886-35-728504; e-mail: tykam@cc.nctu.edu.tw

0020–7683/99/$ - see front matter
PII: S0029–7683(98)00072–9

Table 1
Properties of the Gr/ep laminate

Lamina	
Material Properties	$E_1 = 139.40$ GPa, $E_2 = E_3 = 7.65$ GPa, $G_{12} = G_{13} = 4.35$ GPa $G_{23} = 1.02$ GPa, $v_{12} = v_{13} = 0.29$, $v_{23} = 0.49$
Strengths	$X_T = 1537.2$ MPa, $X_C = 1722.4$ MPa, $Y_T = Z_T = 42.7$ MPa $Y_C = Z_C = 213.9$ MPa, $R = 79.7$ MPa, $S = T = 102.4$ MPa
Thickness	$t = 0.121$ mm
Layups	$[45^\circ_3/0^\circ_3/-45^\circ_3/90^\circ_3]_S$, $[45^\circ_2/0^\circ_3/-45^\circ_2/0^\circ_3/45^\circ_2]_S$, $[(0^\circ_4/90^\circ_4)_2]_S$ $[0^\circ_6/90^\circ_6]_S$, $[45^\circ_6/-45^\circ_6]_S$, $[0^\circ/90^\circ_2/0^\circ_9]_S$, $[45^\circ/-45^\circ_2/45^\circ_9]_S$

laminated composite plates based on classical lamination theory. Reddy and his associates (1987, 1992) used the finite element method, formulated on the basis of first-order shear deformation theory, to calculate the linear and nonlinear first-ply failure loads of laminated composite plates on the basis of several phenomenological failure criteria. Kam and his associates (1995a, 1995b, 1996) studied the linear and nonlinear first-ply failure strengths of cross-ply laminated composite plates using both theoretical and experimental approaches.

In this paper, the previously proposed finite element for thick cross-ply laminates (Kam and Jan, 1995b) is modified and extended to the first-ply failure analysis of generally laminated composite plates. Experimental investigation of first-ply failure strength of laminated composite plates subjected to different loading conditions is performed using an acoustic emission technique. The accuracy of the proposed analytical method in predicting the first-ply failure strength of laminated composite plates is verified by the experimental data.

2. Experimental investigation

A number of square (100×100 mm or 50×50 mm) laminated composite plates with different lay-ups were made of graphite/epoxy [Gr/ep(T300/2500)] prepreg tape supplied by the Torayca Co., Japan. The properties of the Gr/ep material, determined from experiments in accordance with the relevant ASTM standards (1990), and the lay-ups of the plates are listed in Table 1. The experimental apparatus for first-ply failure testing consisted of a load application system, a linear vertical displacement transducer (LVDT), a number of strain gauges, an acoustic emission (AE) system (AMSY4) with two AE sensors, a data acquisition system, and a fixture for clamping the specimens. The AMSY4 was a two-channel AE system manufactured by Vallen System GmbH, Germany. The analogue measurement chain of each channel consisted of an AE sensor, a pre-amplifier and an acoustic signal preprocessor (ASIPP) located in the system case. The AE sensor picked up the stress wave from the specimen and converted it into an electric signal which was then amplified by the preamplifier. In the ASIPP, the AE signal received from the preamplifier was converted into a digital data stream. AE features such as arrival time, duration, peak amplitude, energy, etc. were extracted by a field programmable gate array on the ASIPP and then used for the identification of first-ply failure load. It is noted that at least four AE sensors must be used if

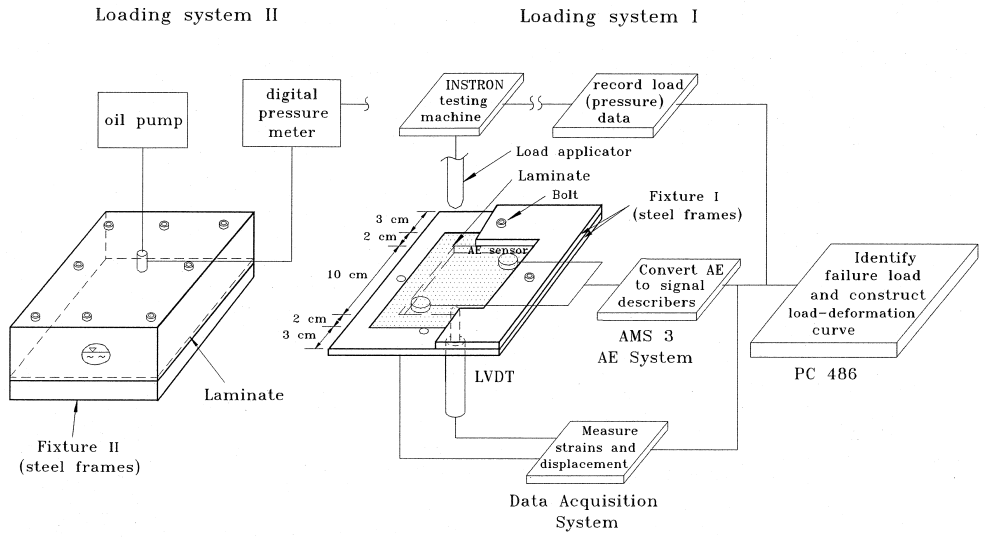

Fig. 1. A sketch of the experimental setup.

the exact failure location is to be identified. Two types of load, namely, a centre-point load and a uniform load, were used in the tests. For the case of the centre point load, the load application system consisted of a 10-ton Instron testing machine and a steel load applicator with a spherical head. The fixture used to clamp the plate was made of two steel frames which were connected together by four bolts. During testing, with the load applicator acting at the centre of the plate, stroke control was adopted to determine the load-deflection relation for the specimens. The loading rate was slow enough for inertia effects to be neglected. For the uniform load case, the load application system consisted of an oil pump and a digital pressure gauge which was connected to the data acquisition system. The fixture for clamping the specimen consisted of a steel frame and a hollow steel box. The specimen was clamped between the steel frame and the box using eight bolts. The diameter of the bolts was 8 mm and the magnitude of the torque used for tightening the bolts was 18.5 Nm. The fixture was sealed to prevent oil leakage. A sketch of the experimental setup is shown in Fig. 1. During testing, the stress waves produced in the specimen were recorded with the AMSY4 (AE) system using the two AE sensors attached to the specimen. The measured acoustic emissions were converted by the AE system to a set of signal parameters, e.g., such as peak amplitude, energy, rise time and duration, which were then used to identify the first-ply failure load of the specimen. For instance, the load–energy and load–cumulative energy diagrams produced by the AE system for the centrally loaded $[45_3^\circ/0_3^\circ/-45_3^\circ/90_3^\circ]_S$ and $[45_2^\circ/0_3^\circ/-45_2^\circ/0_3^\circ/45_2^\circ]_S$ plates are shown in Figs 2–5; the load–energy and load–cumulative energy diagrams for the plates subjected to a uniform load are shown in Figs 6–9. It is noted that the first-ply failure loads of the plates can be easily identified from the above diagrams.

Although the AE system with only two sensors was unable to identify the exact failure locations in the laminated composite plates, positioning the sensors at appropriate points on the specimen could provide an indication of the initial failure location. For a centrally loaded laminated plate, placing the two sensors at different points on one of the two diagonals of the plate pointed to the

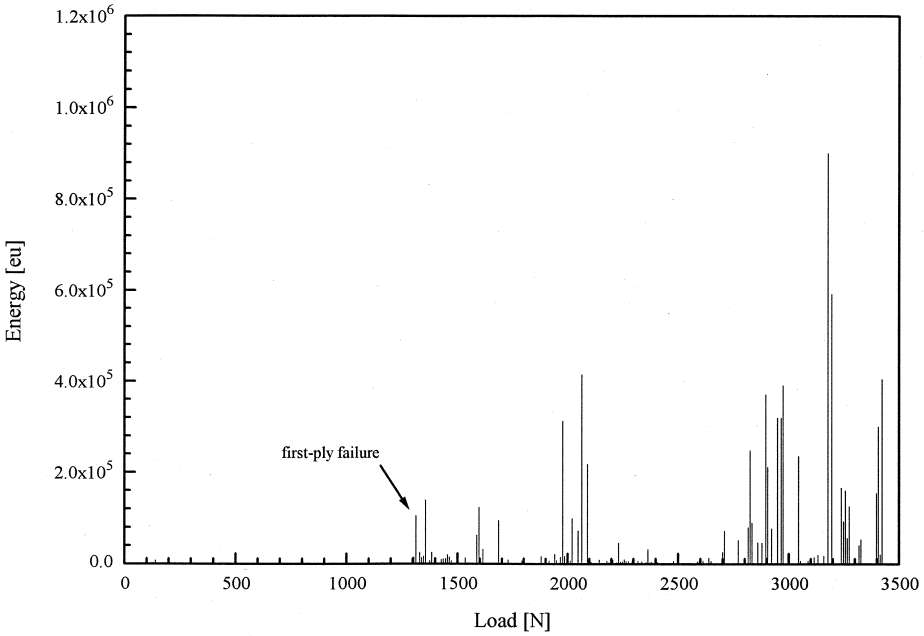

Fig. 2. Load vs energy diagram for the centrally loaded $[45^\circ_3/0^\circ_3/-45^\circ_3/90^\circ_3]_S$ plate.

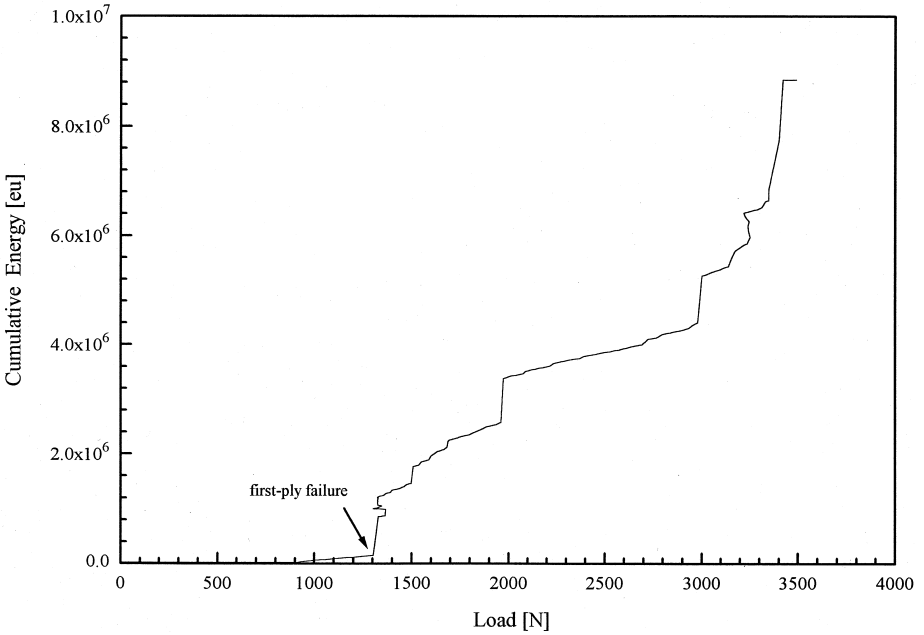

Fig. 3. Load vs cumulative energy diagram for the centrally loaded $[45^\circ_3/0^\circ_3/-45^\circ_3/90^\circ_3]_S$ plate.

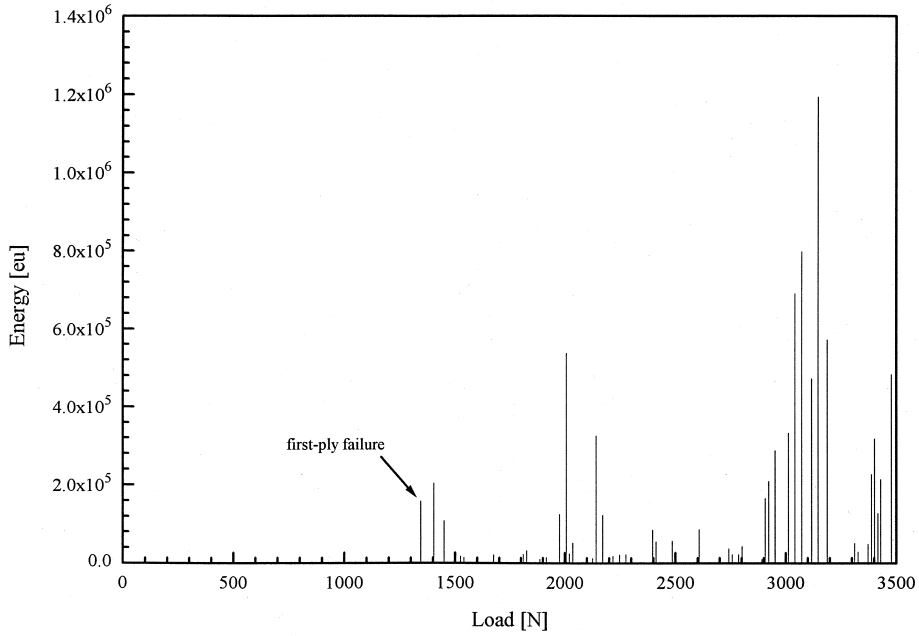

Fig. 4. Load vs energy diagram for the centrally loaded $[45^\circ_2/0^\circ_3/-45^\circ_2/0^\circ_3/45^\circ_2]_S$ plate.

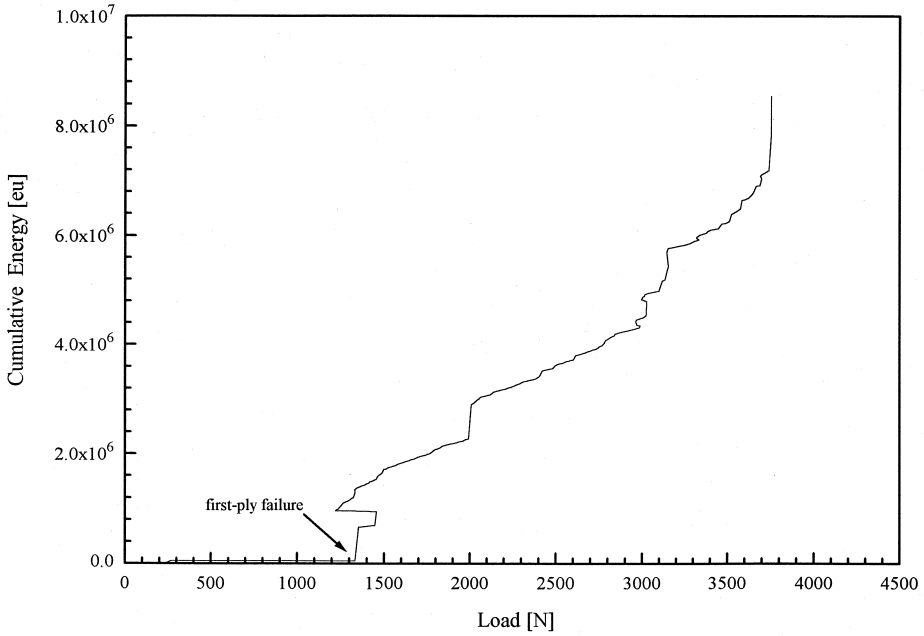

Fig. 5. Load vs cumulative energy diagram for the centrally loaded $[45^\circ_2/0^\circ_3/-45^\circ_2/0^\circ_3/45^\circ_2]_S$ plate.

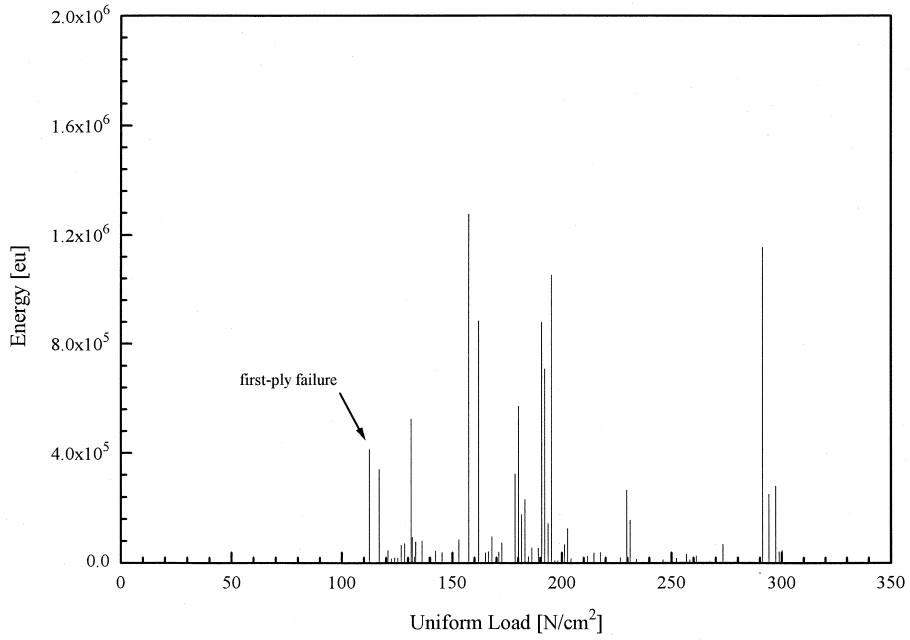

Fig. 6. Load vs energy diagram of uniformly loaded $[45_3^\circ/0_3^\circ/-45_3^\circ/90_3^\circ]_S$ plate.

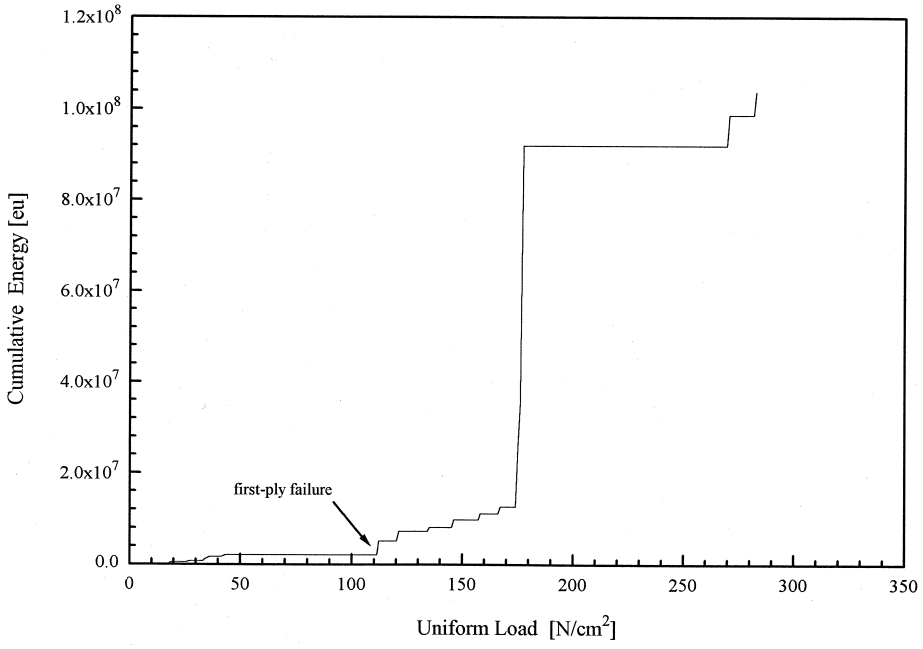

Fig. 7. Load vs cumulative energy diagram for the uniformly loaded $[45_3^\circ/0_3^\circ/-45_3^\circ/90_3^\circ]_S$ plate.

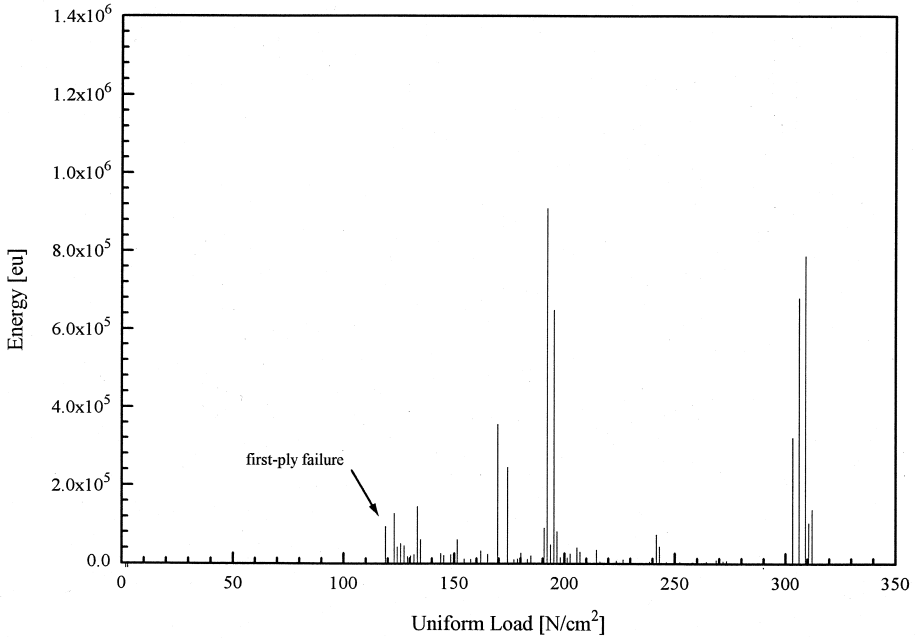

Fig. 8. Load vs energy diagram for the uniformly loaded $[45^\circ_2/0^\circ_3/-45^\circ_2/0^\circ_3/45^\circ_2]_S$ plate.

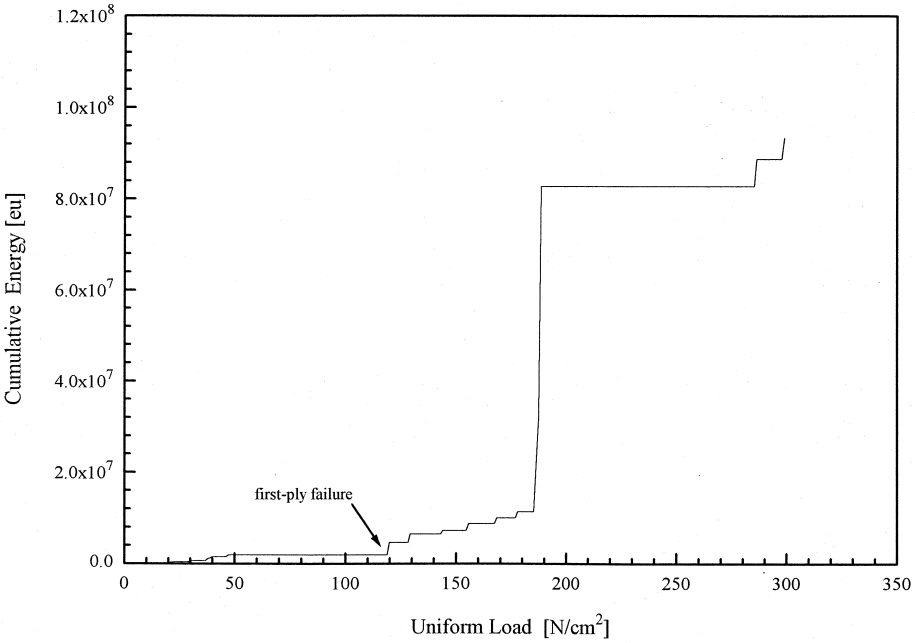

Fig. 9. Load vs cumulative energy diagram for the uniformly loaded $[45^\circ_2/0^\circ_3/-45^\circ_2/0^\circ_3/45^\circ_2]_S$ plate.

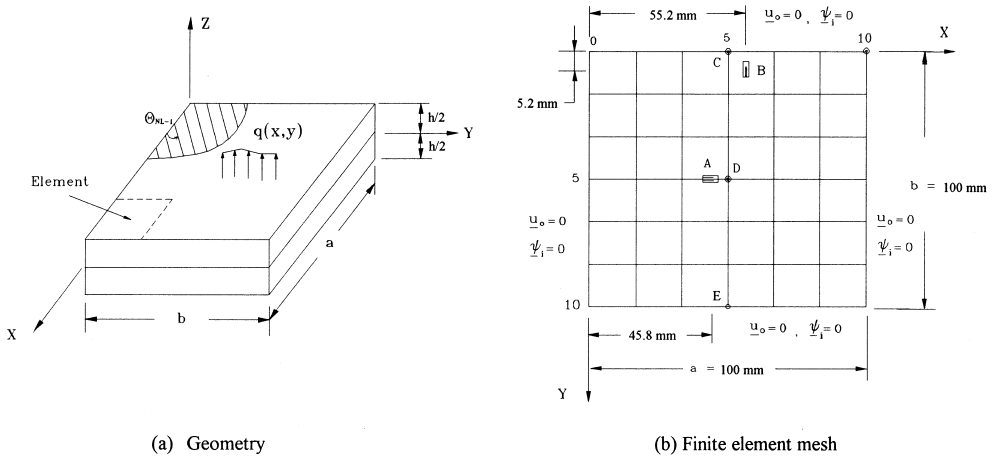

(a) Geometry (b) Finite element mesh

Fig. 10. Laminated composite plate.

centre of the plate as the failure location. On the other hand, placing the two sensors symmetrically about the mid-span of a uniformly loaded plate, identified the mid-point of one of the two edges, which were perpendicular to the line connecting the two sensors, as the failure location. In fact, the failure locations of the laminated composite plates identified by the AE system using the aforementioned technique, were validated by prominent cracks observed on the bottom surface of the plates. It is worth noting that due to symmetry, failure is supposed to initiate at two different but symmetric locations simultaneously in the uniformly loaded laminated composite plate. Nevertheless, experimental observations showed that failure only initiated at one location rather than two in the uniformly loaded plates and the cause of this is attributed to the imperfections in the material.

3. Theoretical approach

The first-ply failure strength of the laminated composite plates tested will be determined using an analytical technique. Consider the laminated composite plate ($a \times b \times h$) composed of a number of orthotropic layers of equal thickness as shown in Fig. 10. The x and y coordinate plane lies in the mid-plane of the plate. It has been shown that for laminated composite plates with aspect ratios $a/h < 10$ or low shear moduli, the effects of shear deformation may become significant and need to be considered in the plate analysis (Ochoa and Reddy, 1992). Herein, the previously proposed finite element method (Kam and Jan, 1995b), which was formulated for cross-ply plates on the basis of a layerwise linear displacement theory, will be modified and extended to the analysis of laminated composite plates with arbitrary layups. Herein, the laminated plate is divided into a number of layer groups through the plate thickness and the displacement components of each layer group are assumed to vary linearly. Each layer group may contain a number of plies which have the same orientation angles. A brief description of the layerwise linear displacement theory is given as follows:

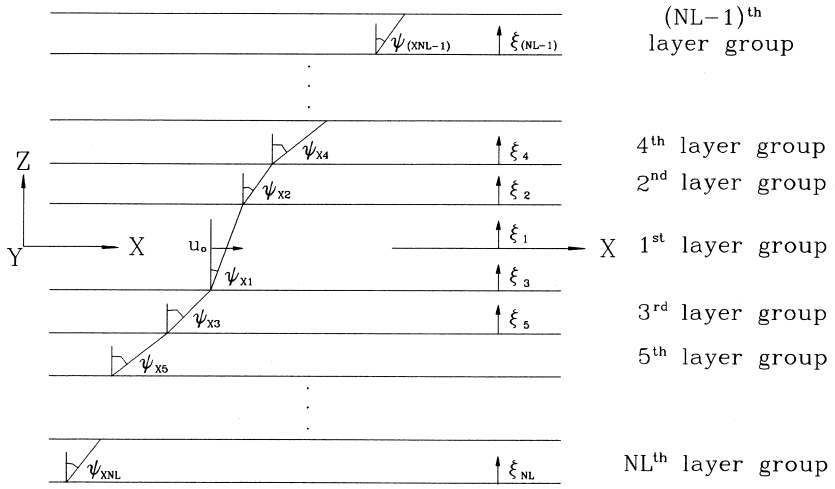

Fig. 11. Layerwise displacement components and local coordinates of layer groups.

$$\mathbf{u}_1 = \mathbf{u}_0 + \xi_1 \boldsymbol{\psi}_1$$

and

$$\mathbf{u}_i = \mathbf{u}_0 + \frac{t_1}{2}\boldsymbol{\psi}_1 + \sum_{k=2,4,\ldots}^{i-2} t_k \boldsymbol{\psi}_k + \xi_i \boldsymbol{\psi}_i \quad (i = 2, 4, 6, \ldots, NL-1)$$

$$\mathbf{u}_i = \mathbf{u}_0 - \frac{t_1}{2}\boldsymbol{\psi}_1 + \sum_{k=3,5,\ldots}^{i-2} t_k \boldsymbol{\psi}_k + \xi_i \boldsymbol{\psi}_i \quad (i = 3, 5, 7, \ldots, NL) \tag{1}$$

where $\mathbf{u}_i = (u, v, w)^t$ is the vector of displacements of the i-th layer group; ξ_i is the local through-thickness coordinate for the i-th layer group; u_0 is the displacement vector in the mid-plane; $\boldsymbol{\psi}_i = (\psi_{xi}, \psi_{yi}, \psi_{zi})^t$ is the vector of rotational degrees of freedom of the i-th layer group; NL is number of layer groups; t_i is the thickness of the i-th layer group. It is noted that no summation is performed in the above equations if (i-2) is less than k. Figure 11 shows the positive directions of ξ_i and ψ_{xi} together with the displacements of the layer groups through the plate thickness in the x-direction.

Three-dimensional stress-strain and strain-displacement relations of the linear theory of elasticity are used to derive the laminated composite finite element on the basis of the principle of minimum total potential energy. In the finite element formulation, the plate is discretized into a number of elements which are connected together at the nodes of the layer groups of elements. The displacements at any point in each layer group are obtained by interpolation using the layer nodal displacements and the appropriate shape functions.

$$\mathbf{u}_0 = \mathbf{N}\bar{\mathbf{u}} \quad i = 1, 2, 3, \ldots, NL$$
$$\boldsymbol{\psi}_i = \mathbf{N}\overline{\boldsymbol{\psi}_i} \tag{2}$$

where $\mathbf{N}$ is a $3 \times ND$ shape function matrix; $\overline{(.)}$ denotes a layer group nodal displacement vector; ND is the number of layer group nodes. Herein, the element stiffness matrix is constructed using a biquadratic ($ND = 9$) formulation of the Lagrange family in which different numerical integration schemes are used for layer groups with different layups. For 0° or 90° layer groups, 3×3 and 2×2 Gauss rules are used for mid-plane displacements and layer rotations, respectively. In contrast to this, 2×2 and 3×3 Gauss rules for mid-plane displacements and layer rotations, respectively, are used for layer groups with arbitrary fibre angles, except 0° and 90°. It is noted that the numerical integration scheme for 0° and 90° layer groups when used for the analysis of a laminated composite plate composed of layer groups with arbitrary fibre angles will overestimate its stiffness as well as first-ply failure load. In the stress analysis, the stresses at the four corner nodes of an element are derived from those at the 2×2 integration points using the following extrapolation equations,

$$\sigma^{i+5} = \left(1+\frac{\sqrt{3}}{2}\right)\sigma^{i+1} + \left(1+\frac{\sqrt{3}}{2}\right)\sigma^{3-i} - 0.5(\sigma^2+\sigma^4) \quad i = 0, 2$$

$$\sigma^{i+6} = \left(1+\frac{\sqrt{3}}{2}\right)\sigma^{i+2} + \left(1+\frac{\sqrt{3}}{2}\right)\sigma^{4-i} - 0.5(\sigma^1+\sigma^3) \quad i = 0, 2 \tag{3}$$

where $\sigma^i (i = 1, \ldots, 4)$ are the stresses at the integration points; $\sigma^i (i = 5, \ldots, 8)$ are the corresponding stresses at the corner nodes. It is noted that if the fibre angles of any two neighbouring layer groups are different, the stresses at the interface between the layer groups will violate the equilibrium conditions, i.e.,

$$\sigma_{zi}^{k,a} \neq \sigma_{zi}^{k+1,b} \quad i = x, y, z \tag{4}$$

where σ_{zi} are the stress components in the plane perpendicular to the z-axis; the superscripts k, a, b denote the layer group number, the top surface and the bottom surface, respectively. For simplicity, the averages of the stresses at the interface of the two neighbouring layer groups are treated as the interfacial stresses σ_{zi}, i.e.,

$$\sigma_{zi} = \tfrac{1}{2}(\sigma_{zi}^{k,a} + \sigma_{zi}^{k+1,a}) \quad i = x, y, z \tag{5}$$

As shown in the following failure analysis, the interfacial stresses do not play an important role in the first-ply failure of laminated composite plates induced by matrix cracking. Nevertheless, the consideration of six independent stress components in the formulation enables the present finite element to analyse laminated plates with complex failure modes. The stresses determined in eqn (5) together with the other stresses obtained in the finite element analysis are then used to evaluate the first-ply failure load P_c of the laminated composite plate on the basis of Tsai–Wu criterion (Tsai and Hahn, 1980) which can be expressed as

$$F_i\sigma_i + F_{ij}\sigma_i\sigma_j \geqslant 1 \quad 1 = 1, 2, \ldots, 6 \tag{6}$$

with

$$F_1 = \frac{1}{X_T} - \frac{1}{X_C}; \quad F_2 = \frac{1}{Y_T} - \frac{1}{Y_C}; \quad F_3 = \frac{1}{Z_T} - \frac{1}{Z_C}$$

$$F_{11} = \frac{1}{X_T X_C}; \quad F_{22} = \frac{1}{Y_T Y_C}; \quad F_{33} = \frac{1}{Z_T Z_C}$$

$$F_{44} = \frac{1}{R^2}; \quad F_{55} = \frac{1}{S^2}; \quad F_{66} = \frac{1}{S^2}$$

$$F_{12} = -\frac{1}{2\sqrt{X_T X_C Y_T Y_C}}; \quad F_{13} = -\frac{1}{2\sqrt{X_T X_C Z_Z Y_C}}; \quad F_{23} = -\frac{1}{2\sqrt{Y_T Y_C Z_T Z_C}} \tag{7}$$

otherwise

$$F_i = F_{ij} = 0$$

where σ_1, σ_2, σ_3 are normal stress components; σ_4, σ_5, σ_6 are shear stress components; X_T, Y_T, Z_T (X_C, X_C, Z_C) are the lamina normal tension (compression strengths in the 1, 2, 3 directions and R, S are the shear strengths in the 23 and 12 planes, respectively. In the above failure criterion, the shear strengths in the 12 and 13 planes are assumed to be the same and $Y_T = Z_T$. Failure locations in the laminated composite plates will be indicated via the reference co-ordinate system shown in Fig. 10.

For comparison purposes, the shear deformable finite element (Kam and Chang, 1993), which was constructed on the basis of first order shear deformation theory (FSDT), is modified and used to predict the first-ply failure strength of the laminated composite plates. Herein, the element stiffness matrix of a generally laminated composite plate is derived using a biquadratic (9 nodes) formulation of the Lagrange family in which 2×2 and 3×3 Gauss rules of numerical integration schemes are used for in-plane displacements and out-of-plane rotations, respectively. For cross-ply plates, the numerical integration schemes with 3×3 and 2×2 Gauss rules are used instead for the in-plane displacements and out-of-plane rotations, respectively.

4. Results and discussion

The accuracy with which the present multilayer finite element predicts deformations of the test specimens is first verified against the experimental results. The finite element mesh and boundary conditions of the laminated composite plates are shown in Fig. 10b. The convergence of the finite element method has been studied using different finite element meshes and numbers of layer groups. It has been found that the use of a 6×6 finite element mesh and around seven to nine layer groups yields reasonably good results for laminated plates. Strains ε_x and ε_y at points A and B, respectively, were measured with strain gauges. The experimental and theoretical load-strain relations of the centrally loaded $[45^\circ_2/0^\circ_3/-45^\circ_2/0^\circ_3/45^\circ_2]_S$ and $[45^\circ_3/0^\circ_3/-45^\circ_3/90^\circ_3]_S$ plates at point A are shown in Figs 12 and 13, respectively, for comparison. It is noted that the use of seven and nine layer groups in the $[45^\circ_3/0^\circ_3/-45^\circ_3/90^\circ_3]_S$ and $[45^\circ_2/0^\circ_3/-45^\circ_2/0^\circ_3/45^\circ_2]_S$ plates, respectively, in the finite element analyses, yields reasonably good results when compared with the experimental data. Further increase in the number of layer groups only gives a slight improvement in the theoretical results. The experimental and theoretical load-strain relations for the uniformly loaded $[45^\circ_2/0^\circ_3/-45^\circ_2/0^\circ_3/45^\circ_2]_S$ and $[45^\circ_3/0^\circ_3/-45^\circ_3/90^\circ_3]_S$ plates at point B are shown in Figs 14 and 15,

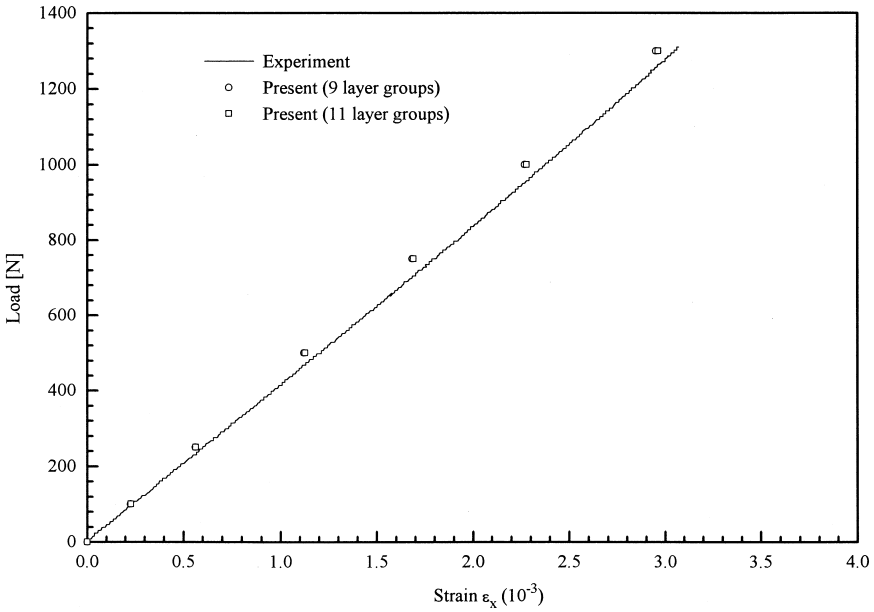

Fig. 12. Load-strain relation of the centrally loaded $[45^\circ_2/0^\circ_3/-45^\circ_2/0^\circ_3/45^\circ_2]_S$ plate.

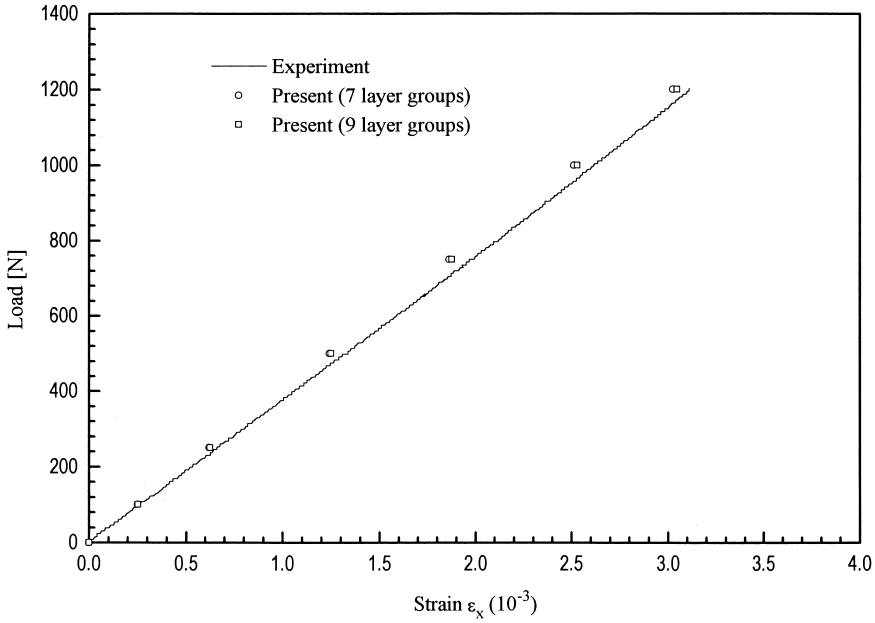

Fig. 13. Load-strain relation of the centrally loaded $[45^\circ_3/0^\circ_3/-45^\circ_3/90^\circ_3]_S$ plate.

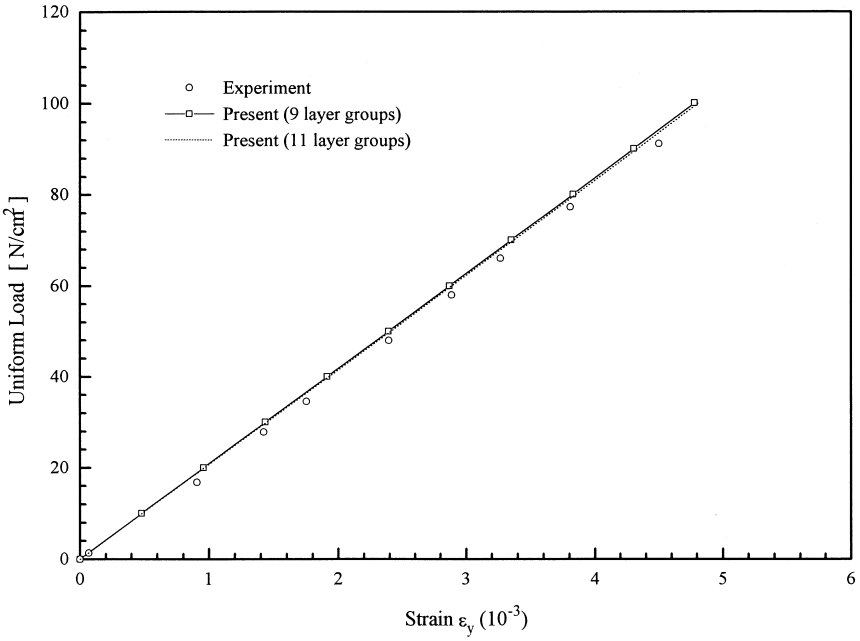

Fig. 14. Load-strain relation of the uniformly loaded $[45^\circ_2/0^\circ_3/-45^\circ_2/0^\circ_3/45^\circ_2]_S$ plate.

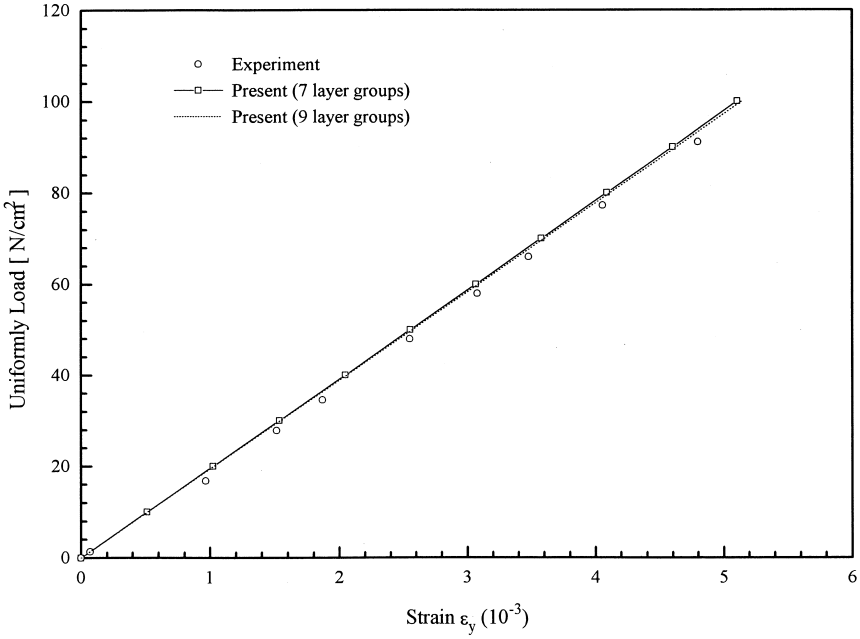

Fig. 15. Load-strain relation of the uniformly loaded $[45^\circ_3/0^\circ_3/-45^\circ_3/90^\circ_3]_S$ plate.

respectively. Again the use of seven and nine layer groups gives reasonably good predictions of the experiment data.

The present multilayer finite element and the shear deformable finite element, together with Tsai–Wu failure criterion, are used to determine the first-ply failure strengths of the laminated composite plates which have been tested. The properties listed in Table 1 are used in the analysis. First, consider the failure analysis of the square laminated composite plates with $a = 100$ mm. The experimental and theoretical first-ply failure strengths together with the theoretically predicted failure locations of the uniformly loaded $[45^\circ_3/0^\circ_3/-45^\circ_3/90^\circ_3]_S$, $[45^\circ_2/0^\circ_3/-45^\circ_2/0^\circ_3/45^\circ_2]_S$ and $[(0^\circ_4/90^\circ_4)_2]_S$ plates and of the centrally loaded $[45^\circ_2/0^\circ_3/-45^\circ_2/0^\circ_3/45^\circ_2]_S$, $[0^\circ_6/90^\circ_6]_S$, $[45^\circ_6/-45^\circ_6]_S$, $[0^\circ/90^\circ_2/0^\circ_9]_S$ and $[45^\circ/-45^\circ_2/45^\circ_9]_S$ plates are listed in Tables 2 and 3, respectively. The aspect ratios of the above laminated composite plates are $a/h = 34.4$ except the $[(0^\circ_4/90^\circ_4)_2]_S$ plate, which is $a/h = 25.8$. It is noted that the present finite element provides more accurate results than the shear deformable finite element when compared with the experimental data. In particular, the use of more layer groups in the present multilayer finite element yields more accurate results. For instance, the first-ply failure loads of the centrally loaded $[0^\circ_6/90^\circ_6]_S$ and $[45^\circ_6/-45^\circ_6]_S$ plates are determined using the following arrangements of layer groups: $[0^\circ_3/0^\circ_3/90^\circ_6/0^\circ_3/0^\circ_3]$, $[45^\circ_3/45^\circ_3/-45^\circ_6/45^\circ_3/45^\circ_3]$, $[0^\circ_2/0^\circ_2/0^\circ_2/90^\circ_6/0^\circ_2/0^\circ_2/0^\circ_2]$, $[45^\circ_2/45^\circ_2/45^\circ_2/-45^\circ_6/45^\circ_2/45^\circ_2/45^\circ_2]$. As listed in Table 3, the use of seven rather than five-layer groups for the plates yields more accurate results. The overall errors of the present finite element in predicting first-ply failure load are less than 2.8% for the cases considered while those of the shear deformable finite element may be as large as 14.7%. As shown in Table 2, although only two specimens were tested for each layup, it is still worth noting that the variations of the experimental first-ply failure loads are small and in general less than 2%. In the theoretical failure analysis, failure is predicted to initiate at point D on the bottom surfaces of the centrally loaded laminated composite plates as shown in Fig. 10b and the theoretical failure locations have been confirmed by experimental observations, i.e., prominent matrix cracks were observed at these locations. For the uniformly loaded laminated plates, failure is predicted to initiate at both points C and E on the plates as shown in Fig. 10b and the theoretical failure locations of the plates are indicated in Table 2. Again the theoretical failure location of the $[(0^\circ_4/90^\circ_4)_2]_S$ plate has been confirmed by experimental observations, i.e., a prominent matrix crack was observed at either points C or E. Finally, consider the failure analysis of the square laminated composite plates with $a = 50$ mm. The experimental and theoretical first-ply failure loads together with the theoretically predicted failure locations of the centrally loaded $[45^\circ_6/-45^\circ_6]_S$, $[0^\circ/90^\circ_2/0^\circ_9]_S$ and $[45^\circ/-45^\circ_2/45^\circ_9]_S$ plates are listed in Table 4. The comparison between the plates with the same layups in Tables 3 and 4 shows that the errors of the present finite element in predicting first-ply failure loads remain small (less than 2%) while those of the shear deformable finite element go up as the aspect ratio of the plates decreases from 34.4 to 17.2. The failure locations of the plates also remain unchange irrespective of the aspect ratio of the plates. The failure mode of the uniformly or centrally loaded laminated composite plates is matrix cracking. In the theoretical study, it has been found that the effects of the stresses in the Z-direction (through thickness direction) on the first-ply failure of the laminated plates are minimal and thus the neglection of these stresses in the failure analysis does not have a significant effect on the magnitude of the theoretical first-ply failure load of the plates, i.e., the percentage change in first-ply load is less than 1%. Nevertheless, the inclusion of the through thickness stresses in the failure analysis is vital for laminated composite plates subjected to complex loading condition or with delamination being a major failure mode.

Table 2
First-ply failure strength of uniformly loaded laminated composite plates ($a = 100$ mm)

Plate		First-ply failure strength (MPa)					Difference		Failure location			
		Theoretical		Experimental								
				Specimen								
Layup	No. of layer groups	I Present	II FSDT	A	B	III $(A+B/2)$	$\lvert(\text{III}-\text{I}/\text{III})\rvert \times 100$	$\lvert(\text{III}-\text{II}/\text{III})\rvert \times 100$	Point	X (mm)	Y (mm)	Z (mm)
$[45^\circ_3/0^\circ_3/-45^\circ_3 90^\circ_3]_S$	7	1.16	1.27	1.11	1.14	1.13	2.7	12.4	C	50	0	+1.089
									E	50	100	+1.089
$[45^\circ_2/0^\circ_3/-45^\circ_2/0^\circ_3 45^\circ_2]_S$	9	1.20	1.35	1.18	1.19	1.19	0.8	13.4	C	50	0	+1.21
									E	50	100	+1.21
$[(0^\circ_4/90^\circ_4)_2]_S$	7	1.85	2.10	1.82	1.83	1.83	1.1	14.8	C	50	0	+1.936
									E	50	100	+1.936

Table 3
First-ply failure load of centrally loaded laminated composite plates ($a = 100$ mm)

Plate		First-ply failure load (N)							Difference (%)		Failure location			
		Theoretical		Experimental (III)										
				Specimens										
Layup	No. of layer groups	Present (I)	FSDT (II)	1	2	3	4	Average	$\lvert(\text{III}-\text{I}/\text{III})\rvert\times 100$	$\lvert(\text{III}-\text{II}/\text{III})\rvert\times 100$	Point	X (mm)	Y (mm)	Z (mm)
$[45^\circ_3/0^\circ_3/-45^\circ_3/90^\circ_3]_S$	7	1322	1443	1309	1315	1319	1321	1316	0.4	9.7	D	50	50	−1.452
$[45^\circ_2/0^\circ_3/-45^\circ_2/0^\circ_3/45^\circ_2]_S$	9	1373	1528	1334	1340	1351	1355	1345	2.1	13.6				
$[0^\circ_6/90^\circ_6]_S$	5	1327	1412	1289	1293	1296	1299	1294	2.6	9.1				
	7	1319	—						2.0	—				
$[45^\circ_6/-45^\circ_6]_S$	5	1353	1413	1309	1319	1321	1323	1318	2.6	7.3				
	7	1347	—						2.2	—				
$[0^\circ/90^\circ_2/0^\circ_9]_S$	5	1998	2018	1956	1958	1966	1973	1963	1.8	2.8				
$[45^\circ/-45^\circ_2/45^\circ_9]_s$	5	2061	2098	2025	2034	2035	2038	2033	1.4	3.2				

Table 4
First-ply failure load of centrally loaded laminated composite plates ($a = 50$ mm)

Plate		First-ply failure load (N)							Difference (%)		Failure location			
		Theoretical		Experimental (III)										
				Specimens										
Layup	No. of layer groups	Present (I)	FSDT (II)	1	2	3	4	Average	$\lvert(\text{III}-\text{I}/\text{III})\rvert\times 100$	$\lvert(\text{III}-\text{II}/\text{III})\rvert\times 100$	Point	X (mm)	Y (mm)	Z (mm)
$[45^\circ_6/-45^\circ_6]_S$	5	1285	1390	1259	1261	1264	1272	1264	1.7	10.1	D	25	25	−1.452
	7	1282	—						1.4	—				
$[0^\circ/90^\circ_2/0^\circ_9]_S$	5	1708	1797	1682	1688	1694	1701	1691	1.0	6.3				
$[45^\circ/-45^\circ_2/45^\circ_9]_S$	5	1742	1838	1709	1718	1728	1732	1722	1.1	6.8				

5. Conclusions

First-ply failure strengths of several laminated composite plates with different layups under various loading conditions were determined using experimental and analytical techniques. An acoustic emission technique was used to detect the stress waves emitted from the failure sources in the laminated plates and the first-ply failure loads of the plates were determined from the load–energy diagrams constructed from the measured acoustic emissions. The previously proposed finite element, formulated on the basis of a layerwise linear displacement theory, was modified and extended to the first-ply failure analysis of laminated composite plates. Theoretical first-ply failure strengths of the plates were determined with the present finite element together with the Tsai–Wu failure criterion. Comparisons between the experimental and theoretical first-ply failure strengths of the laminated composite plates with different aspect ratios were made. Good agreement between the theoretical and experimental results demonstrates that the present analytical method predicts the first-ply failure strength of generally laminated composite plates reasonable accurately. The laminated composite finite element formulated on the basis of the first order shear deformation theory may be inappropriate for the finite analysis of moderately thick laminated composite plates.

Acknowledgements

This research was supported by the National Science Council of the Republic of China under Grant No. NSC 85-2212-E009-019. Their support is gratefully appreciated.

References

ASTM Standards and Literature References for Composite Material, 2nd ed., 1990.

Kam, T.Y., Chang, R.R., 1993, Finite element analysis of shear deformable laminated composite plates. Journal of Energy Resource Technology, ASME 115, 41–46.

Kam T.Y., Sher, H.F., 1995a, Nonlinear and first-ply failure analysis of laminated cross-ply plates. Journal of Composite Materials 29, 463–482.

Kam, T.Y., Jan, T.B., 1995b, First-ply failure analysis of laminated composite plates based on the layerwise linear displacement theory. Journal of Composite Structures 32, 583–591.

Kam, T.Y., Chang, R.R., Sher, H.F., Chao, T.N., 1996, Prediction of first-ply failure strengths of laminated composite plates using a finite element approach. International Journal of Solids and Structures 33, 375–398.

Ochoa, O.O., Reddy, J.N., 1992, Finite Element Analysis of Composite Laminates. Kluwer Academic Publishers, Dordrecht.

Reddy, J.N., Pandey, A.K., 1987, A first-ply failure analysis of composite laminates. Computers and Structures 25, 371–393.

Reddy, Y.S.N., Reddy, J.N., 1992, Linear and non-linear failure analysis of composite laminates with transverse shear. Comp. Sci. Tech. 44, 227–255.

Tsai, S.W., Hahn, H.T., 1980, Introduction to Composite Materials. Technomic Publishing Co., Lancaster, PA.

Turvey, G.J., 1980a, An initial flexural failure analysis of symmetrically laminated cross-ply rectangular plates. Int. J. Solids Struct. 16, 451–463.

Turvey, G.J., 1980b, Flexural failure analysis of angle-ply laminates of GFRP and CFRP. J. Strain Anal. 15, 43–49.

Turvey, G.J., 1980c, A study of the onset of flexural failure in cross-ply laminated strips. Fibre Sci. Technol. 13, 325–336.

Turvy, G.J., 1981, Initial flexural failure of square, simply supported, angle-ply plates. Fibre Sci. Technol. 15, 47–63.